Different roles for ApcD and ApcF in Synechococcus elongatus and Synechocystis sp. PCC 6803 phycobilisomes

Pablo I Calzadilla, Fernando Muzzopappa, Pierre Sétif, Diana Kirilovsky

Different roles for ApcD and ApcF in Synechococcus elongatus and Synechocystis sp. PCC 6803 phycobilisomes

Pablo I. Calzadilla, Fernando Muzzopappa, Pierre Sétif, Diana Kirilovsky

PII: S0005-2728(19)30037-4
DOI: https://doi.org/10.1016/j.bbabio.2019.04.004
Reference: BBABIO 48021

To appear in: *BBA - Bioenergetics*

Received date: 23 February 2018
Revised date: 20 December 2018
Accepted date: 6 January 2019

Please cite this article as: P.I. Calzadilla, F. Muzzopappa, P. Sétif, et al., Different roles for ApcD and ApcF in Synechococcus elongatus and Synechocystis sp. PCC 6803 phycobilisomes, BBA - Bioenergetics, https://doi.org/10.1016/j.bbabio.2019.04.004

Different roles for ApcD and ApcF in *Synechococcus elongatus* and *Synechocystis sp.* PCC 6803 phycobilisomes

Pablo I Calzadilla, Fernando Muzzopappa, Pierre Sétif and Diana Kirilovsky

Affiliations

Institute for Integrative Biology of the Cell (I2BC), CEA, CNRS, Université Paris-Sud, Université Paris-Saclay, 91198 Gif sur Yvette, France

Corresponding author: Diana Kirilovsky, diana.kirilovsky@cea.fr, Tel: 33 1 69089571; Fax: 33 1 69088717; Institute for Integrative Biology of the Cell (I2BC), CEA, CNRS, Université Paris-Sud, Université Paris-Saclay, 91198 Gif sur Yvette, France

Abstract

The phycobilisome, the cyanobacterial light harvesting complex, is a huge phycobiliprotein containing extramembrane complex, formed by a core from which rods radiate. The phycobilisome has evolved to efficiently absorb sun energy and transfer it to the photosystems via the last energy acceptors of the phycobilisome, ApcD and ApcE. ApcF also affects energy transfer by interacting with ApcE. In this work we studied the role of ApcD and ApcF in energy transfer and state transitions in *Synechococcus elongatus* and *Synechocystis* PCC6803. Our results demonstrate that these proteins have different roles in both processes in the two strains. The lack of ApcD and ApcF inhibits state transitions in *Synechocystis* but not in *S. elongatus*. In addition, lack of ApcF decreases energy transfer to both photosystems only in *Synechocystis*, while the lack of ApcD alters energy transfer to photosystem I only in *S. elongatus*. Thus, conclusions based on results obtained in one cyanobacterial strain cannot be systematically transferred to other strains and the putative role(s) of phycobilisomes in state transitions need to be reconsidered.

Keywords: phycobilisome, cyanobacteria, state transition, energy transfer

1. Introduction

Plants, algae and cyanobacteria, by harvesting solar energy and converting it into chemical energy, provide food and oxygen that are essential for life on earth. In eukaryotic (plants and algae) and prokaryotic (cyanobacteria) oxygen-evolving organisms, photosynthesis involve the participation of two photosystems operating in series, formed by the photochemical centers and antennae, the light harvesting complexes. While the membrane-bound photochemical centers (including the water-oxidizing complex) are similar in cyanobacteria, algae and plants, a large diversity of antennae appeared along evolution. Two major groups can be distinguished: the membrane-bound light-harvesting complexes (LHCII and LHCI), which binds chlorophylls and carotenoids and are present in green algae and in plants, and the huge extramembrane phycobilisomes (PBSs) which bind bilins and are present in red algae, glaucophytes and cyanobacteria (with the exception of prochlorophytes).

Antennae have evolved to efficiently harvest energy in a large variety of ecological niches and environmental conditions. However, when energy absorption exceeds the rate of carbon fixation, light can become lethal since dangerous reactive oxygen species are generated. Thus, oxygenic photosynthetic organisms have developed photoprotective mechanisms in which the efficient light-harvesting antennae enters into quenching states, in which the excess excitation energy is converted into heat. Due to the diversity of antennae, these mechanisms also differ in LHC-containing and PBS-containing organisms (reviews [1-3]). In plants and green algae, this photoprotective state is induced by acidification of the thylakoid lumen (under high light conditions), triggering protonation of PbsS, a Photosystem II (PSII) subunit, and LHCII, and inducing conformational changes in this complex (reviews [4-6]). The acidic lumen also induces the synthesis of zeaxanthin from violaxanthin, via the xanthophyll cycle [7, 8]. By contrast, in cyanobacteria, strong blue-green light photoactivates a soluble carotenoid protein: the Orange Carotenoid Protein (OCP). The photoactivated protein thermally dissipates the excess of excitation light absorbed by PBSs, through its interaction with them [9, 10]. In red algae, the PBS seems not to be involved in thermal dissipation of excess energy [11-13].

The LHCII is also involved in “State transitions”, a mechanism that in plants and green algae controls the relative extent of energy arriving at one or the other reaction center, avoiding an over-reduction or over-oxidation of the intersystem electron transport chain [14]. In this mechanism, two states are defined: State I, which presents a high PSII to Photosystem I (PSI) fluorescence ratio (and is induced by light preferentially absorbed by PSI), and State

II, characterized by a low PSII to PSI fluorescence ratio (and induced by light preferentially absorbed by PSII). Reduction of the PQ pool and binding of PQH_2 at the Qo site of the cyt b_6f activate a specific kinase which phosphorylates some LHCII trimers [15]. Phosphorylation induces LHCII detachment from PSII and partial (or total) attachment to PSI, triggering the transition to State II [16, 17]. Meanwhile, dephosphorylation of LHCII triggers the opposite phenomenon and transition to State I (see review [18]).

The role of PBS in cyanobacteria state transitions is less clear. Several models were proposed for the molecular mechanism of cyanobacterial state transitions. One model considers that PBS movement induces changes in direct energy transfer to PSII and PSI [19-21], such as it was demonstrated for LCHII in plant and alga state transitions [22, 23]. In another model called the "spillover model", the energy transfer from PBS to PSII remains equal in both states, but the excess of energy absorbed by PSII is transferred to PSI in State II (spillover). Spillover was proposed to involve movement of photosystems [24-31]. Lastly, in a recent study, it was proposed that the fluorescence changes in cyanobacterial state transitions are due to a PSII-related quenching in State II, without involvement of spillover and with a little participation of PBS detachment [32]. Nevertheless, the prevalence of one mechanism over the other, or the co-existence of some/all of them, is still a matter of discussion.

The PBSs, attached to the stromal side of the thylakoids, are formed by phycobiliproteins (PBPs) (covalently binding linear tetrapyrrole chromophores, the bilins) and linker proteins (mostly non-chromophorylated). The PBPs absorb solar energy and the linker proteins have principally a structural role. The highly ordered structure of the PBS, formed by a core (close to the membranes) from which rods radiate, ensures directional energy transfer with high quantum yield, from the rods to the core and finally to the reaction centers (Figure 1) (for reviews, see [33-35]).

The rods, which are formed by two to four stacked PBPs hexamers, can contain only phycocyanin (PC, blue) hexamers in most of fresh water strains (like those used in this study: *Synechococcus elongatus* PCC 7942 (hereafter *S. elongatus*) and *Synechocystis* sp. PCC 6803 (hereafter *Synechocystis*)) or PC plus phycoerythrin (PE, red to violet) in marine strains. Meanwhile, the core is formed by two (*S. elongatus*), three (*Synechocystis*) or five (*Nostoc* PCC 7120) cylinders, each composed of 4 trimers of allophycocyanin (APC, blue). Furthermore, each APC trimer is formed by αAPC-βAPC heterodimers. In the basal cylinders, which are in contact with the membranes, each trimer has a different composition (Figure 1C). Trimer 1 is formed by 3 α/β APC dimers containing the linker-core (Lc) protein

in the central hole. Trimer 2 is a pure α/β APC trimer. Trimer 3 contains one α/β APC dimer, one dimer formed by an αAPC subunit and ApcF (a βAPC-like subunit) and finally a dimer formed by a βAPC subunit and the bilin-linker domain of ApcE. The bilins attached to ApcF and ApcE are close (20 Å) and have big influences one on the other. In trimer 4, which also contains the Lc linker protein, one α APC subunit is replaced by ApcD. ApcE and ApcD bilins are also relatively close although they are in different APC trimers.

While the APC trimers containing only αAPC-βAPC heterodimers have a fluorescence maximum at 660 nm, the trimers containing ApcD and ApcE/ApcF emit at 680 nm. ApcE and ApcD transfer the energy absorbed by the PBS to the photosystems. ApcE is also essential for the integrity of the PBS core and the interaction of the PBS with the membrane [36]. The PBS can transfer the absorbed energy to both photosystems. Several models exist showing the interaction of one hemi-discoidal PBS with a PSII dimer [37-39], whereas its interaction with PSI is less clear due to the protuberance of stromal extra-membrane PSI subunits. The energy arriving at each reaction center depends on the cyanobacterial strain and also on environmental conditions: while in *Arthrospira platensis* 80% of absorbed energy arrives to PSI [40], this drops to 50% in *Synechocystis*[41].

It was shown that in *Synechococcus* PCC 7002, lack of ApcD decreases energy transfer from PBS to PSI and lack of ApcF decreases energy transfer to PSII. Thus, it was concluded that ApcD is essential for energy transfer to PSI while the lack of ApcF largely impairs energy transfer to PSII [42, 43]. However, analysis of 77 K and room temperature fluorescence in *Synechocystis* suggested that energy transfer from PBSs to both photosystems, is largely affected in the absence of ApcF but only a little in the absence of ApcD [44].

In addition, the absence of ApcD and ApcF affects state transitions. The ΔApcD mutants of *Synechocystis*, *Synechococcus* PCC 7002 and *Anabaena sp.* PCC 7120 lack state transitions [42, 44-46]. These cells present a high PSII fluorescence in darkness and under blue and orange illumination, which is related to State I [42, 44, 45]. It was proposed that this phenotype was due to the lack of energy transfer from PBSs to PSI [42] and/or a permanent PBS binding to PSII [44] in the ΔApcD mutant. Meanwhile, the lack of ApcF inhibits state transitions in *Synechocystis* [44] but not in *Synechococcus* PCC 7002 [42, 44].

The contradictory results already obtained in the ApcD and ApcF *Synechocystis* and *Synechococcus* 7002 mutants, with regard to energy transfer and state transitions, suggested that the role of these proteins could be different in different strains [42-44]. However, none of these studies directly compared the strain-dependence effect of these mutations. To further

understand the role of these proteins, we compared in the present study the phenotype of ΔApcD and ΔApcF mutants of *S. elongatus* and *Synechocystis* cells. We show that lack of these proteins alters the energy transfer from PBSs to PSII and PSI in different ways in these strains. Surprisingly, the lack of ApcD or ApcF was found to not impair state transitions in *S. elongatus*.

2. Materials and Methods

2.1 Culture conditions

The cyanobacteria *Synechocystis* sp. PCC 6803 and *Synechococcus elongatus* PCC 7942, wild-type (WT), ΔApcD and ΔApcF strains were grown photo-autotrophically in BG11 medium [47]. Cells were kept in a rotary shaker (120 rpm) at 31 °C and illuminated by fluorescence white lamps (50 µmol photons m^{-2} s^{-1}) under a CO_2-enriched atmosphere (50 mL/min CO_2 flow into the incubator). Cells were maintained in their logarithmic phase of growth for all the experiments. The *Synechocystis* ΔApcD, ΔApcF and ApcE-C190S strains were obtained by [48], and the CK mutant strain from [49].

2.2 ΔApcD and ΔApcF *S. elongatus* mutants construction

To construct the ΔApcD mutant, a 2.2 kb DNA region surrounding the *Synpcc7942_0240* locus, encoding the *apcD* gene, was amplified by PCR using genomic DNA of *S. elongatus*. The two restriction sites-creating oligonucleotides used (XhoI_apcD_fw and NotI_apcD_rv) are presented in Supplementary Table S1. The resulting PCR product was digested by NotI and XhoI restriction enzymes and cloned in the pBluescript SK+ plasmid. Then, the plasmid was digested by SmaI and ligated to a 1.3 kb kanamycin resistance cassette, interrupting the *apcD* gene. This plasmid was named "*interrupted apcD"*

To construct the ΔApcF mutant, a 1.2 kb DNA region surrounding the *Synpcc7942_2158* locus, encoding the *apcF* gene, was amplified using genomic DNA of *S. elongatus*. The two restriction sites-creating oligonucleotides (XhoI_apcF_fw and NotI_apcF_rv) are shown in Supplementary Table S1. The resulting PCR product was digested by NotI and XhoI restriction enzymes and cloned in the pBluescript SK+ plasmid. A new SmaI restriction site was introduced 240 pb downstream of the ApcF start-codon, by site directed mutagenesis, using the Quickchange XL kit of Stratagene and the oligonucleotides ApcF_smaI_fw and ApcF_smaI_rv (Supplementary Table S1). An enzymatic digestion by

SmaI and BstAPI was used to replace the initial 200 nucleotides of *apcF* gene by a spectomycin/streptomycin (Sm/Sp) resistance cassette, inactivating the *apcF* gene. This plasmid was called *ΔapcF* since it lacks a large portion of the *apcF* gene

The "*interrupted apcD"* and Δ*apcF* plasmids were used to transform *S. elongatus* as described in [50]. Selection was made at 33°C and under dim light (30 µmol photons m^{-2} s^{-1}), on plates containing BG11 medium supplemented with 1% agarose and different antibiotics: 40 µg/mL kanamycin or 25 µg/mL spectomycin and 50 µg/mL streptomycin (for ΔApcD and ΔApcF, respectively). Genomic DNA was isolated from the colonies growing in the presence of antibiotics as described in [50]. PCR analysis and DNA sequencing were performed in order to confirm complete segregation (Supplementary Figure S1).

2.3 LC-MS/MS analysis

To confirm the absence of ApcD in the PBSs of the ΔApcD mutant, a LC-MS/MS analysis was performed. PBS isolation was performed as described in [51]. The isolated PBSs of WT and ΔApcD *S. elongatus* strains were diluted in 50 mM NH_4HCO_3 for enzymatic digestion. Then, peptides were analyzed by LTQ-Orbitrap Velos for the identification of the ApcD protein in the samples. Measurements were done by the SICaPS service of the Institut de Biologie Intégrative de la Cellule (I2BC), Gif-sur-Yvette, France.

2.4 Fluorescence measurements

2.4.1 PAM fluoremeter

State transitions were monitored using a pulse amplitude modulated fluorometer (101/102/103-PAM; Walz, Effeltrich, Germany), in a 1x1 cm square stirred cuvette. All experiments were carried at 31°C on dark-adapted (15 min) whole cells at a chlorophyll concentration of 2.5 µg/mL. State I was induced by 85 µmol photons m^{-2} s^{-1} of blue-green light (halogen white light filtered by a Corion cut-off 550-nm filter; 400 to 500 nm). State II was induced by 25 µmol photons m^{-2} s^{-1} of orange light (halogen white light filtered by a Melles Griot 03 FIV 046 filter; 600 to 640 nm) or by dark incubation. Saturating flashes (400 ms x 1200 µmol photons m^{-2} s^{-1}) were given to probe the maximum fluorescence level. The fluorescence parameters used in the analysis are the following: F_0, basal fluorescence; F_{md}, maximum fluorescence in darkness; $F_{m'}$, maximum fluorescence under illumination; F_{mb}, maximum fluorescence under blue light illumination; F_{mo}, maximum fluorescence under

orange light illumination; F_v = variable fluorescence = F_m-F_0; F_{vd}, variable fluorescence in darkness; F_{vb}, variable fluorescence under blue light illumination.

2.4.2 Fluorescence Emission spectra

77 K and room temperature fluorescence emission spectra were monitored in a CARY Eclipse spectrophotometer (Varian). For 77 K measurements, whole cells (5.0 μg Chl/mL) were dark-adapted for 15 min before the measurements. Then, spectra were recorded corresponding to State II. For State I spectra, cells were illuminated for 5 min by 85 μmol photons m^{-2} s^{-1} of blue-green light (halogen white light filtered by a Corion cut-off 550-nm filter; 400 to 500 nm). Samples were collected in RMN tubes (5 mm diameter) and frozen by immersion in liquid nitrogen. Excitation was made at 430 nm or 590 nm, and emission was scanned from 620 nm to 800 nm. All spectra were normalized by the signal intensity at 800 nm.

Room temperature fluorescence spectra were recorded at a phycocyanin concentration of 1 μM, estimated using the formulae expressed in [52]. Whole cells were dark-adapted for 15 min before the measurements, which corresponds to State II conditions. Excitation was made at 590 nm and emission was scanned from 620 nm to 800 nm.

2.4.3 Closure of PSII reaction centers

The closure of reaction centers was followed by the PSI fluorometer (PSI Instruments, Brno, Czech Republic), in the 1-ms to 1-s time range, in dark-adapted (15 min) whole cells (2.5 μg Chl/mL). Before the measurements, DCMU (10 μM) and DBMIB (20 μM) were added to the cells. Blue measuring light (λ = 460 nm) and orange actinic light (35 μmol photons m^{-2} s^{-1}, λ = 630 nm) were used in all cases.

2.5 $P700^+$ measurements

P700 absorption changes were measured using the P700 module of a standard PAM (101/102/103-PAM; Walz, Effeltrich, Germany). Measurements were made at 31 °C on whole cells (2.5 μg Chl/mL) in a 1x1 cm square cuvette in the presence of DCMU (15 μM), DBMIB (100 μM) and methyl viologen (MV, 300 μM). Orange light (halogen white light filtered by a Melles Griot 03 FIV 046 filter; 600 to 640 nm) or blue light (halogen white light filtered by a Corion cut-off 550-nm filter; 400 to 500 nm) were used as actinic lights.

3. Results and discussion

3.1 Energy transfer from PBS to photosystems in the *S. elongatus* and *Synechocystis* ΔApcD and ΔApcF mutants

The construction of the *Synechocystis* ΔApcD and ΔApcF mutants was described in [48]. The construction of the *S. elongatus* mutants is described in Materials and Methods. The phycocyanin (PC, absorbance at 620 nm) to chlorophyll (Chl, absorbance at 680 nm) ratio was higher in *S. elongatus* than in *Synechocystis* cells~~, showing that the PBS to photosystems ratio is larger in *S. elongatus*~~ (Figure 2). While the PC to Chl ratio was similar between the mutants and WT *S. elongatus* cells, the ΔApcF *Synechocystis* mutant always presented a slightly smaller PC to Chl ratio. The PSI to PSII ratio was also measured in both WT strains by $(F_A, F_B)^-$ and $TyrD^+$ EPR signals, being 2-3 in *S. elongatus* and 4-5 in *Synechocystis*.

Room temperature fluorescence spectra of all strains presented a maximum at 660 nm (related to bulk APC) and a shoulder at 680 nm (related to PBS terminal emitters, ApcD and ApcE, and PSII Chl) (Figure 2C and D). ΔApcD and ΔApcF mutants showed a higher fluorescence at 660 nm (at the same PC concentration) than the WT, in *S. elongatus* as well as in *Synechocystis* cells. This could be related to a defective energy transfer from PBS to one photosystem or the other (or to both photosystems) and/or to a defective energy transfer from bulk APC to terminal emitters and/or a different state in darkness. It is important to remark that while in *Synechocystis*, the highest fluorescence was observed in the ΔApcF mutant, in *S. elongatus*, the ΔApcD mutant showed the highest fluorescence. These results already suggest that the lack of these proteins has different effects on energy transfer in the two strains.

To investigate whether the PSII effective antenna size varies in the ΔApcD and ΔApcF *S. elongatus* and *Synechocystis* mutants, their fluorescence induction curves in the presence of DCMU and DBMIB were compared to those of their respective WTs. When adding DCMU, the rate of fluorescence increase depends only on the antenna size and it is independent of the dark PQ pool redox state and light PQ reoxidation rate. DBMIB was added to avoid State I transition during the measurements. Figure 3 shows the kinetics of fluorescence induction induced by non-saturating orange light (preferentially absorbed by phycobiliproteins) in dark-adapted WT and mutants cells of *S. elongatus* and *Synechocystis*. The fluorescence induction kinetics in the ΔApcD *Synechocystis* and *S. elongatus* cells, compared to their respective WTs, were almost identical (Figure 3), indicating that the absence of ApcD does not affect energy transfer from PBS to PSII in neither of these strains. In contrast, the absence of ApcF slowed down the kinetics of fluorescence induction in *Synechocystis* cells, but not in *S. elongatus* (Figure 3). Thus, the absence of ApcF seems to affect energy transfer from PBS to

PSII only in *Synechocystis* cells, with multiphasic kinetics suggesting some heterogeneity in the coupling of PBS to PSII (see discussion below).

Then, to investigate whether the absence of ApcD or ApcF affects the energy transfer from PBS to PSI, we measured the oxidation kinetics of P700 in the presence of DCMU (15 µM), DBMIB (100 µM) and MV (300 µM) (Figure 4). The presence of DCMU prevents the reduction of $P700^+$ by electrons coming from PSII. DBMIB inhibits reduction of lumenal electron donors by cyclic/respiratory electron transport and, in addition, MV largely inhibits charge recombination in PSI. In the presence of these inhibitors, P700 photo-oxidation exhibits no or a negligible lag phase. This indicates that lumenal electron donors are preoxidized in darkness, due presumably to cytochrome oxidase activity. Under these conditions, the initial rate of P700 photooxidation depends only on the antenna size. The measurements were done using orange or blue actinic light (Figure 4 and Supplementary Figure S2, respectively).

Under blue light illumination, the kinetics of P700 oxidation were rather similar in WT and mutants strains. This was expected since the Chl antennae were not modified in these mutants (Supplementary Figure S2). In contrast, under orange light illumination, the rates of P700 oxidation were slower in the ΔApcD *S. elongatus* and the ΔApcF *Synechocystis* mutants, than in their respective WTs (Figure 4 and Table I). Therefore, less energy transfer from PBS to PSI occurred in these strains (Figure 4A and D). By contrast, no significant differences were observed in the rates of P700 oxidation in the ΔApcD *Synechocystis* and the ΔApcF *S. elongatus* mutants, when compared to their respective WTs (Table I, Figure 4B and C).

Altogether, these experiments show that the absence of ApcD does not affect energy transfer to PSII in any of the strains studied (*Synechocystis* and *S. elongatus* (this work) and *Synechococcus* PCC7002 [43]), indicating that ApcE is either the major energy donor to PSII or can replace ApcD in this role when ApcD is absent. In agreement with these results, several structural studies showed the interaction of the ApcE-containing trimer with the PSII reaction center and its internal antenna [38, 39, 53]. In contrast to what happens in the absence of ApcD, the lack of ApcF affects the energy transfer from PBS to PSII in *Synechocystis* (this work) and *Synechococcus* PC7002 [42], but not in *S. elongatus*. Nevertheless, the decrease of energy transfer observed is smaller than that induced by a modification of the bilin-binding Cys in ApcE (Supplementary Figure S3). In this mutant, the bilin is not attached covalently to the protein and it has an emission at 710 nm instead of at 680 nm [48]. This bilin acts as a competitive trap of the energy absorbed by the PBS. Interestingly, the PBSs having this modified ApcE are still able to transfer energy to PSII with a rather high efficiency,

suggesting that in this case energy transfer occurs principally via ApcD. The rate of closure of PSII centers (increase of fluorescence) was largely faster in the ApcE *Synechocystis* mutant than in a mutant in which the PBSs lack the rods (CK strain) (Supplementary Figure S3).

The lack of ApcF also affects the energy transfer from PBSs to PSI in *Synechocystis* (this work and [44]), but neither in *S. elongatus* (this work), nor in *Synechococcus* PCC 7002 [43]. As already said, in trimer 3 of the basal core cylinders, one β subunit and an α subunit from different dimers are replaced by ApcF and the bilin-binding domain of ApcE, respectively (Figure 1). The bilins attached to ApcF and ApcE are close (20 Å) and have big influences one on the other. In the ΔApcF mutant, ApcF is replaced by a βAPC subunit. This replacement seems to be very well tolerated in *S. elongatus* PBSs with no changes in energy transfer to any of the photosystems. By contrast, in *Synechocystis* and *Synechococcus* PCC 7002, this change decreases the energy transfer to photosystems, most probably by modifying the interaction between the bilins.

On the contrary, the lack of ApcD affects energy transfer to PSI in *S. elongatus* and *Synechococcus* PCC 7002 but not in *Synechocystis*. This result was unexpected in *Synechocystis* since Liu et al 2013 [39] showed that, in this strain, ApcD can be cross-linked with PSI polypeptides, suggesting its localization on the edge area of PSI. Nevertheless, it has been already suggested that ApcD plays a secondary role (if any) in energy transfer to photosystems in *Synechocystis* [44]. Our results and those of Ashby and Mullineaux do not allow us to discard the possibility that ApcD transfers energy to PSI in WT *Synechocystis*. However, they clearly demonstrate that in the absence of ApcD, energy transfer to both photosystems is not decreased indicating that ApcE can efficiently transfer the energy absorbed by the PBS to both photosystems. In *S. elongatus* and *Synechococcus* PCC 7002, ApcE can also transfer energy to PSI but less efficiently than ApcD. We can conclude that in different cyanobacteria strains, the role of PBS terminal emitters in energy transfer and/or the structure of the core PBS and/or the interaction PBS/photosystems are different. Thus, the results obtained in one strain cannot be simply extrapolated to all cyanobacteria strains.

3.2 State transitions in WT and ApcD and ApcF mutants of *S. elongatus* and *Synechocystis*

As we already mentioned, it was reported that the lack of ApcD inhibits state transitions in *Synechocystis*, *Synechococcus* PCC 7002 and *Anabaena* PCC 7120 [42, 44-46]. In addition, the ΔApcF *Synechocystis* mutant also seemed to be affected in state transitions

[44]. In this work, we studied the effect of the lack of these proteins in *S. elongatus* and *Synechocystis*.

3.2.1 Fluorescence kinetics at room temperature followed by a PAM fluorimeter

Fluorescence changes induced by illumination in dark-adapted WT and mutated *S. elongatus* and *Synechocystis* cells were followed at room temperature by a PAM fluorimeter. Figure 5 shows typical traces of fluorescence kinetics in dark-adapted *S. elongatus* (Figure 5A) and *Synechocystis* (Figure 5B) cells, successively illuminated by low intensities of blue and orange light. Dark-adapted cells presented a low maximal fluorescence (F_{md}) indicating that cells were in State II. This is typical for cyanobacteria cells in which the PQ pool is reduced in darkness by the respiratory electron transport chain [54]. Upon illumination with blue light, preferentially exciting chlorophyll, a large and rapid increase of F_m' was observed (arriving to a maximal F_{mb}' level), indicating transition to State I. The F_{vb} to F_{vd} ratio (F_v = variable fluorescence = F_m-F_0) was around 4.7 in WT *S. elongatus* while being only 1.2 in WT *Synechocystis* cells (Figure 5, Table II). Under orange illumination (preferentially exciting phycobiliproteins) of blue-light adapted cells, a decrease of F_m' in both cyanobacterial strains was induced (Figure 5). In *Synechocystis* cells, the steady state F_{mo} level was similar to the F_{md} level, while in *S. elongatus* the F_{mo} level was higher.

Figure 5C and E show the variation of fluorescence induced by successive blue and orange illuminations in dark-adapted ΔapcD and ΔapcF *S. elongatus* mutants, respectively. Blue illumination of these cells induced a large and rapid increase of F_m'. Then, illumination by orange light reduced the F_m' value, in a manner equivalent to that observed for WT *S. elongatus* cells. The fluorescence parameters of different independent experiments were averaged and are shown in Table II. Comparison of the F_{vb} to F_{vd} ratio in the three strains indicates that the absence of ApcD or ApcF did not affect state transitions in *S. elongatus* (Table II). By contrast, the lack of ApcD completely abolished state transitions in *Synechocystis* (Figure 5D). The absence of ApcF in the same strain, although it did not completely suppressed state transitions, largely decreased the amplitude of fluorescence changes (Figure 5F).

3.2.2 State transitions studied by 77 K fluorescence spectra

The 77 K fluorescence emission spectra were measured in WT and mutants cells of *S. elongatus* and *Synechocystis* cells after dark incubation (15 min, State II) and blue light illumination (5 min, State I) (Figures 6 and 7). When the PBSs were preferentially excited in

WT cells (excitation at 590 nm), we observed a large peak at 650-660 nm related to PC and APC fluorescence, a peak at 683 nm related to CP43 and the last emitters of PBS, a peak (or shoulder) at 695 nm corresponding to Reaction Center II and CP47, and finally a peak at 718-725 nm related to PSI fluorescence [55, 56]. The PSII-related peaks at 683 and 695 nm were higher in blue-light adapted cells (State I) than in dark-adapted cells (State II), showing the typical fluorescence changes related to state transitions in *S. elongatus* and *Synechocystis*.

When the chlorophyll was preferentially excited (excitation at 430 nm), the PSI emission peak (at 718-725 nm) was the highest one. The PSI fluorescence was similar in dark and blue-light adapted cells. The PSII-related peaks at 683 and 695 nm were higher when cells were incubated under illumination than in darkness. It is worth noting that, in *S. elongatus*, the peak at 683 nm could be contaminated with some PBS fluorescence, since an emission peak at 660 nm was observed. The relative sizes of the different peaks (related to PBPs, PSII and PSI) were different in *S. elongatus* and *Synechocystis*, which could be due at least partially to differences in PBP to Chl and PSII to PSI ratios. In addition, the differences of 683 and 695 nm emissions between State I and II were much larger in *S. elongatus* than in *Synechocystis.*

When comparing the 77 K fluorescence emission spectra of the WT and mutants cells of *S. elongatus*, some differences were observed (Figure 6 and Supplementary Figure S4). When the excitation was done at 590 nm, the peak at 681-683 nm was largely higher in the ΔApcD mutant than in the WT suggesting a partial functional disconnection of PBSs in the mutant. This is in agreement with the observation that there is less energy transfer from PBS to PSI in this mutant.

In the ΔApcF strain, the 660 nm to 683/695 nm emission ratio was higher than in the WT (Figure 6 and Supplementary Figure S4), although the ratio PC to Chl was similar in both strains (or even slightly lower in the mutant) (Figure 2). This suggests that energy transfer from the bulk APC (emission 660 nm) to terminal PBS emitters could be affected in this mutant. Nevertheless, this decrease in energy transfer must be small since alterations of energy transfer from PBS to photosystems were not detected in the ΔApcF strain. The 77 K spectrum of the ΔApcF *Synechocystis* mutant also presented big differences compared to the WT *Synechocystis* spectrum: the 660 nm to 683/695 nm emission ratio was largely larger in the mutant (Figure 7). This agrees with the affected energy transfer from PBSs to photosystems detected in ΔApcF *Synechocystis* cells.

Both ΔApcD and ΔApcF mutants of *S. elongatus* also presented large differences in 77 K fluorescence emission spectra between dark adapted (State II) and blue-light adapted (State I) conditions (Figure 6C-F). The emission peaks at 683 and 695 nm (PBS and PSII emission) were largely higher in State I (blue-light illumination) than in State II (darkness), not only when the cells were excited at 590 nm but also when excited at 430 nm. The emission increase was similar (or even slightly larger in ΔApcD) in the mutants than in the WT, confirming that the absence of ApcD and ApcF does not affect at all state transitions, as shown by the PAM measurements. The PSI emission peaks were similar in both states. It is worth mentioning that PBSs of the WT and ΔapcD *S. elongatus* strains were isolated to confirm the absence of ApcD in the mutant strain. A LC-MS/MS analysis was carried out and no ApcD protein was detected in the ΔApcD *S. elongatus* PBS, while its presence was confirmed in the WT PBS.

By contrast, in ΔApcD and ΔApcF *Synechocystis* mutants, state transitions were largely affected. In ΔApcD *Synechocystis*, the 695 to 720 nm emission ratio was similar in darkness and under blue illumination indicating complete inhibition of state transitions. In ΔApcF, a slight increase of 695 nm emission was detected but smaller than that observed in the WT indicating partial state transitions inhibition. When ΔApcD and ΔApcF cells were excited at 430 nm, a very small (smaller than in WT) but reproducible fluorescence increase of the 695 nm peak was observed in State I (Figure 7). This confirms previous observations done by other laboratories [44, 46].

From the above results we can hypothesize that PBSs are not or very little involved in *S. elongatus* state transitions, and/or that ApcD has a different role in *S. elongatus*. In the past, it was proposed that the impairment of state transitions in the **Δ**ApcD *Synechocystis* mutant was due to alterations in the relative binding constants between PBSs and photosystems [44]. In its absence, the PBS would remind attached to PSII and the cells would be permanently in State I as suggested by the higher PSII fluorescence in darkness in the mutant. ApcD is located at the bottom of the PBSs core, together with ApcE in adjacent trimers [57]. The replacement of ApcD with an α-APC subunit, could alter the PBS core structure and/or interaction with the membrane affecting PBS movement and/or detachment/attachment. This could occur in *Synechocystis*, *Synechococcus* PCC 7002 and *Anabaena*, but clearly does not occur in *S. elongatus*.

Other authors proposed that the inhibition of state transitions in the ΔApcD mutant was due to the incapacity of the PBS to transfer energy to PSI [42]. Thus, the PBS could

move but the energy transfer to PSI would not increase. The results obtained in *S. elongatus* do not agree with this proposal. The energy transfer from PBSs to PSI is decreased in *S. elongatus* as it is the case in *Synechococcus* PCC7002 [42]. However, while state transitions are inhibited in *Synechococcus* PCC7002, they are not altered in *S. elongatus*.

The deletion of the *rpaC* gene coding a 9 kDa protein localized in the cytoplasmic side of thylakoids also has different effects in *Synechocystis* and *S. elongatus* cells [58-60]. In *Synechocystis*, the lack of this protein inhibits state transitions [58]. It was suggested that RpaC stabilizes the PBS-PSII interaction [60]. In *S. elongatus*, a large decrease of RpaC did not affect state transitions [61]. In this strain, the *rpaC* gene seems to be essential since complete segregation of the mutant was never obtained [61].

State-transitions related fluorescence changes are also observed when Chl is preferentially excited, showing that state transitions also involve processes that take place in membranes. These processes are not inhibited in any of the strains studied in this work. McConnell et al. [46] also showed that in the ΔApcD *Synechococcus sp*. PCC 7002 mutant, small fluorescence differences were observed between States I and II when Chl was excited. These Chl changes are larger in *S. elongatus* than in *Synechocystis* and *Synechococcus* PCC 7002, suggesting that the membrane processes involved in state transitions could be more important in *S. elongatus* than in the other strains. Indeed, Ranjbar et al [32] showed that a large PSII fluorescence quenching (not related to spillover) is involved in *S. elongatus* transition to State II. This quenching was also observed in *Synechocystis* cells, although its amplitude was largely smaller [32].

Using time-resolved fluorescence and streak camera, Chukhutsina et al [62] showed that in *Synechocystis* WT cells, fluorescence changes are mainly related to PBS uncoupling in State I. A very small PBS uncoupling was also observed in *S. elongatus* [32]. The smaller role of PBSs in *S. elongatus* state transitions could partially explain the fact that this process is not inhibited in the ΔApcD mutant. Our results strongly suggest that the relative involvement of PBSs and membrane processes in state transitions could vary in different cyanobacterial strains.

4. Conclusions

The lack of ApcD and ApcF affects differently energy transfer and state transitions in different cyanobacteria strains, indicating that conclusions based on results obtained in one cyanobacterial strain cannot be systematically transferred to other strains. ApcD is clearly

involved in energy transfer from PBS to PSI in *S. elongatus* and in *Synechococcus* PCC7002. In *Synechocystis*, it is either not involved in energy transfer to any of the photosystems or it can be efficiently replaced by ApcE. By contrast, the lack of ApcF affects energy transfer to both photosystems in *Synechocystis* but not in *S. elongatus*. Surprisingly, the lack of ApcD does not hinder state transitions in *S. elongatus* while it inhibits state transitions in all other studied cyanobacterial strains. This could be explained by a different role of ApcD in the interaction between the PBS and the photosystems and/or a different role of PBSs in *S. elongatus* and *Synechocystis* cells. The contribution of membrane processes could be larger in *S. elongatus* than in *Synechocystis* and other studied strains. In any case, the putative roles of PBSs in state transitions need to be reconsidered.

5. Supplementary Material

Supplementary Figure S1. Genotyping of *S. elongatus* mutants.

Supplementary Figure S2. P700 oxidation absorption kinetics under blue illumination of S. elongatus and Synechocystis ΔApcD and ΔApcF mutants.

Supplementary Figure S3. Chlorophyll *a* fluorescence induction transients of *Synechocystis* apcE-C190S and CK strains.

Supplementary Figure S4. Comparison of 77 K fluorescence emission spectra of dark and light adapted WT and mutant S. elongatus cells.

Supplementary Table S1. Primers used in the construction of the Δ*apcD* and Δ*apcF* mutants of *S. elongatus*.

6. Footnotes

Author contributions: P.C. performed most of the experiments and analyzed the data; F.M. constructed the cyanobacterial mutants; P.S. designed, performed, analyzed and supervised experiments; D.K. conceived the project, designed and supervised experiments, analyzed data; the article was written by D.K., P.S. and P.C.

Funding: This work was supported by grants from the Agence Nationale de la Recherche (ANR projects RECYFUEL (ANR-16-CE05-0026); by the European Union's Horizon 2020 research and innovation program under grant agreement no. 675006 (SE2B). P.C. salary is financed by RECYFUEL (ANR project). F.M. salary is financed by SE2B. The research is also supported by the Centre National de la Recherche Scientifique (CNRS) and the Commissariat à l'Energie Atomique (CEA). The French Infrastructure for Integrated Structural Biology (FRISBI) ANR-10-INBS-05 also partially supported this research.

7. References

[1] K.K. Niyogi, T.B. Truong, Evolution of flexible non-photochemical quenching mechanisms that regulate light harvesting in oxygenic photosynthesis, Current opinion in plant biology, 16 (2013) 307-314.
[2] A. Derks, K. Schaven, D. Bruce, Diverse mechanisms for photoprotection in photosynthesis. Dynamic regulation of photosystem II excitation in response to rapid environmental change, Biochim Biophys Acta, 1847 (2015) 468-485.
[3] N.C.M. Magdaong, R.E. Blankenship, Photoprotective, excited-state quenching mechanisms in diverse photosynthetic organisms, J Biol Chem, 293 (2018) 5018-5025.
[4] S. de Bianchi, M. Ballottari, L. Dall'osto, R. Bassi, Regulation of plant light harvesting by thermal dissipation of excess energy, Biochemical Society transactions, 38 (2010) 651-660.
[5] A.V. Ruban, Nonphotochemical Chlorophyll Fluorescence Quenching: Mechanism and Effectiveness in Protecting Plants from Photodamage, Plant Physiol, 170 (2016) 1903-1916.
[6] A.V. Ruban, M.P. Johnson, C.D. Duffy, The photoprotective molecular switch in the photosystem II antenna, Biochim Biophys Acta, 1817 (2012) 167-181.
[7] A.M. Gilmore, H.Y. Yamamoto, Linear-models relating xanthophylls and lumen acidity to nonphotochemical fluorescence quenching - evidence that antheraxanthin explains zeaxanthin-independent quenching, Photosynth Res, 35 (1993) 67-78.
[8] H.Y. Yamamoto, Biochemistry of the violaxanthin cycle in higher plants, Pure Appl Chem, 51 (1979) 639-648.
[9] A. Wilson, G. Ajlani, J.M. Verbavatz, I. Vass, C.A. Kerfeld, D. Kirilovsky, A soluble carotenoid protein involved in phycobilisome-related energy dissipation in cyanobacteria, Plant Cell, 18 (2006) 992-1007.
[10] A. Wilson, C. Punginelli, A. Gall, C. Bonetti, M. Alexandre, J.M. Routaboul, C.A. Kerfeld, R. van Grondelle, B. Robert, J.T. Kennis, D. Kirilovsky, A photoactive carotenoid protein acting as light intensity sensor, Proc. Natl. Acad. Sci. U. S. A., 105 (2008) 12075-12080.
[11] E. Delphin, J.C. Duval, A.L. Etienne, D. Kirilovsky, State transitions or Delta pH-dependent quenching of photosystem II fluorescence in red algae, Biochemistry, 35 (1996) 9435-9445.
[12] E. Delphin, J.C. Duval, D. Kirilovsky, Comparison of state 1 state 2 transitions in the green alga Chlamydomonas reinhardtii and in the red alga Rhodella violacea: Effect of kinase and phosphatase inhibitors, Biochim. Biophys. Acta-Bioenerg., 1232 (1995) 91-95.
[13] T. Krupnik, E. Kotabova, L.S. van Bezouwen, R. Mazur, M. Garstka, P.J. Nixon, J. Barber, R. Kana, E.J. Boekema, J. Kargul, A reaction center-dependent photoprotection mechanism in a highly robust photosystem II from an extremophilic red alga, Cyanidioschyzon merolae, J Biol Chem, 288 (2013) 23529-23542.
[14] C. Bonaventura, J. Myers, Fluorescence and oxygen evolution from Chlorella pyrenoidosa, Biochim Biophys Acta, 189 (1969) 366-383.
[15] F.A. Wollman, C. Lemaire, Studies on kinase-controlled state transitions in Photosystem II and b_6f mutants from *Chlamydomonas Reinhardtii* which lack quinone-binding proteins, Biochimica et biophysica acta, 933 (1988) 85-94.
[16] P. Horton, The effect of redox potential on the kinetics of fluorescence induction in pea chloroplasts. I. Removal of the slow phase, Biochim Biophys Acta, 635 (1981) 105-110.
[17] D.J. Kyle, I. Ohad, C.J. Arntzen, Membrane protein damage and repair: Selective loss of a quinone-protein function in chloroplast membranes, Proc Natl Acad Sci U S A, 81 (1984) 4070-4074.
[18] J. Minagawa, State transitions--the molecular remodeling of photosynthetic supercomplexes that controls energy flow in the chloroplast, Biochim Biophys Acta, 1807 (2011) 897-905.
[19] J.F. Allen, C.E. Sanders, N.G. Holmes, Correlation of membrane-protein phosphorylation with excitation-energy distribution in the cyanobacterium *Synechococcus* 6301, FEBS Lett., 193 (1985) 271-275.

[20] C.W. Mullineaux, J.F. Allen, State 1 - State 2 transitions in the Cyanobacterium *Synechococcus* 6301 are controlled by the redox state of electron carriers between Photosystem I and Photosystem II, Photosynth. Res., 23 (1990) 297-311.
[21] C.W. Mullineaux, M.J. Tobin, G.R. Jones, Mobility of photosynthetic complexes in thylakoid membranes, Nature, 390 (1997) 421-424.
[22] A.V. Vener, P.J. van Kan, P.R. Rich, I. Ohad, B. Andersson, Plastoquinol at the quinol oxidation site of reduced cytochrome bf mediates signal transduction between light and protein phosphorylation: thylakoid protein kinase deactivation by a single-turnover flash, Proc Natl Acad Sci U S A, 94 (1997) 1585-1590.
[23] F.A. Wollman, State transitions reveal the dynamics and flexibility of the photosynthetic apparatus, Embo J, 20 (2001) 3623-3630.
[24] J. Biggins, D. Bruce, Regulation of excitation-energy transfer in organisms containing phycobilins, Photosynth Res, 20 (1989) 1-34.
[25] J. Biggins, N.A. Tanguay, H.A. Frank, Electron-transfer reactions in Photosystem-I following vitamin-K1 depletion by ultraviolet-Irradiation, FEBS Lett., 250 (1989) 271-274.
[26] D. Bruce, J. Biggins, Mechanism of the light-state transition in photosynthesis : V. 77 K linear dichroism of *Anacystis nidulans* in state 1 and state 2, Biochim Biophys Acta, 810 (1985) 295-301.
[27] K. El Bissati, E. Delphin, N. Murata, A. Etienne, D. Kirilovsky, Photosystem II fluorescence quenching in the cyanobacterium *Synechocystis* PCC 6803: involvement of two different mechanisms, Biochim Biophys Acta, 1457 (2000) 229-242.
[28] S. Federman, S. Malkin, A. Scherz, Excitation energy transfer in aggregates of Photosystem I and Photosystem II of the cyanobacterium Synechocystis sp. PCC 6803: Can assembly of the pigment-protein complexes control the extent of spillover?, Photosynth Res, 64 (2000) 199-207.
[29] A.C. Ley, W.L. Butler, Energy distribution in the photochemical apparatus of *Porphyridium cruentum* in State-I and State-II, Biochim. Biophys. Acta., 592 (1980) 349-363.
[30] J. Olive, I. Mbina, C. Vernotte, C. Astier, F.A. Wollman, Randomization of the Ef particles in thylakoid membranes of *Synechocystis* 6714 upon transition from State-I to State-II, FEBS Lett., 208 (1986) 308-312.
[31] C. Vernotte, M. Picaud, D. Kirilovsky, J. Olive, G. Ajlani, C. Astier, Changes in the Photosynthetic Apparatus in the Cyanobacterium Synechocystis Sp Pcc-6714 Following Light-to-Dark and Dark-to-Light Transitions, Photosynthesis research, 32 (1992) 45-57.
[32] R. Ranjbar Choubeh, E. Wientjes, P.C. Struik, D. Kirilovsky, H. van Amerongen, State transitions in the cyanobacterium Synechococcus elongatus 7942 involve reversible quenching of the photosystem II core, Biochim Biophys Acta, 1859 (2018) 1059-1066.
[33] N. Adir, Structure of the phycobilisome antennae in cyanobacteria and red algae, in: P. Fromme (Ed.) Photosynthetic Protein Complexes: A Structural Approach, WILEY-VCH Verlag GmbH & Co. KGaA, Weinheim, 2008, pp. 243-274.
[34] A.N. Glazer, Phycobilisome - a macromolecular complex optimized for light energy-transfer, Biochim Biophys Acta, 768 (1984) 29-51.
[35] R. MacColl, Cyanobacterial phycobilisomes, J Struct Biol, 124 (1998) 311-334.
[36] T. Redlinger, E. Gantt, A M(r) 95,000 polypeptide in *Porphyridium cruentum* phycobilisomes and thylakoids: Possible function in linkage of phycobilisomes to thylakoids and in energy transfer, Proc Natl Acad Sci U S A, 79 (1982) 5542-5546.
[37] A.A. Arteni, G. Ajlani, E.J. Boekema, Structural organisation of phycobilisomes from *Synechocystis* sp. strain PCC6803 and their interaction with the membrane, Biochim Biophys Acta, 1787 (2009) 272-279.
[38] L. Chang, X. Liu, Y. Li, C.-C. Liu, F. Yang, J. Zhao, S.-F. Sui, Structural organization of an intact phycobilisome and its association with photosystem II, Cell research, 25 (2015) 726.
[39] H. Liu, H. Zhang, D.M. Niedzwiedzki, M. Prado, G. He, M.L. Gross, R.E. Blankenship, Phycobilisomes supply excitations to both photosystems in a megacomplex in cyanobacteria, Science, 342 (2013) 1104-1107.

[40] M.G. Rakhimberdieva, V.A. Boichenko, N.V. Karapetyan, I.N. Stadnichuk, Interaction of phycobilisomes with photosystem II dimers and photosystem I monomers and trimers in the cyanobacterium *Spirulina platensis*, Biochemistry, 40 (2001) 15780-15788.
[41] L. Tian, I.H. van Stokkum, R.B. Koehorst, A. Jongerius, D. Kirilovsky, H. van Amerongen, Site, rate, and mechanism of photoprotective quenching in cyanobacteria, Journal of the American Chemical Society, 133 (2011) 18304-18311.
[42] C. Dong, A. Tang, J. Zhao, C.W. Mullineaux, G. Shen, D.A. Bryant, ApcD is necessary for efficient energy transfer from phycobilisomes to photosystem I and helps to prevent photoinhibition in the cyanobacterium Synechococcus sp. PCC 7002, Biochim Biophys Acta, 1787 (2009) 1122-1128.
[43] J.D. Zhao, J.H. Zhou, D.A. Bryant, Energy transfer processes in phycobilisomes as deduced from mutational analyses, Photosynth. Res., 34 (1992) 83-83.
[44] M.K. Ashby, C.W. Mullineaux, The role of ApcD and ApcF in energy transfer from phycobilisomes to PSI and PSII in a cyanobacterium, Photosynth Res, 61 (1999) 169-179.
[45] C. Dong, J. Zhao, ApcD is required for state transition but not involved in blue-light induced quenching in the cyanobacterium *Anabaena* sp. PCC7120, Chi Sci Bull, 53 (2008) 3422-3424.
[46] M.D. McConnell, R. Koop, S. Vasil'ev, D. Bruce, Regulation of the distribution of chlorophyll and phycobilin-absorbed excitation energy in cyanobacteria. A structure-based model for the light state transition, Plant Physiol, 130 (2002) 1201-1212.
[47] M. Herdman, S.F. Delaney, N.G. Carr, A new medium for the isolation and growth of auxotrophic mutants of the blue-green alga *Anacystis nidulans*, J. Gen. Microbiol., 79 (1973) 233-237.
[48] D. Jallet, M. Gwizdala, D. Kirilovsky, ApcD, ApcF and ApcE are not required for the Orange Carotenoid Protein related phycobilisome fluorescence quenching in the cyanobacterium Synechocystis PCC 6803, Biochim Biophys Acta, 1817 (2012) 1418-1427.
[49] G. Ajlani, C. Vernotte, L. Dimagno, R. Haselkorn, Phycobilisome Core Mutants of *Synechocystis* PCC 6803, Biochim Biophys Acta, 1231 (1995) 189-196.
[50] E.M. Clerico, J.L. Ditty, S.S. Golden, Specialized techniques for site-directed mutagenesis in cyanobacteria, Methods in molecular biology, 362 (2007) 155-171.
[51] M. Gwizdala, A. Wilson, D. Kirilovsky, *In vitro* reconstitution of the cyanobacterial photoprotective mechanism mediated by the Orange Carotenoid Protein in *Synechocystis* PCC 6803, Plant Cell, 23 (2011) 2631-2643.
[52] J. Myers, J.R. Graham, R.T. Wang, Light Harvesting in Anacystis nidulans Studied in Pigment Mutants, Plant Physiol, 66 (1980) 1144-1149.
[53] J. Barber, E.P. Morris, P.C. da Fonseca, Interaction of the allophycocyanin core complex with photosystem II, Photochem Photobiol Sci, 2 (2003) 536-541.
[54] M. Aoki, S. Katoh, Oxidation and reduction of plastoquinone by photosynthetic and respiratory electron transport in a cyanobacterium *Synechococcus* sp, Biochim. Biophys. Acta, 682 (1982) 307-314.
[55] D. Siefermann-harms, Fluorescence properties of isolated chlorophyll-protein complexes, in: H. Lichtenthaler (Ed.) Application of chlorophyll fluorescence, Kluwer Academic Publisher, Dordrecht, The Netherlands, 1988, pp. 45-54.
[56] R.J. Vandorssen, J.J. Plijter, J.P. Dekker, A. Denouden, J. Amesz, H.J. Vangorkom, Spectroscopic properties of chloroplast grana membranes and of the core of Photosystem-II, Biochim. Biophys. Acta., 890 (1987) 134-143.
[57] J. Zhang, J. Ma, D. Liu, S. Qin, S. Sun, J. Zhao, S.F. Sui, Structure of phycobilisome from the red alga Griffithsia pacifica, Nature, 551 (2017) 57-63.
[58] D. Emlyn-Jones, M.K. Ashby, C.W. Mullineaux, A gene required for the regulation of photosynthetic light harvesting in the cyanobacterium Synechocystis 6803, Mol Microbiol, 33 (1999) 1050-1058.
[59] S. Joshua, C.W. Mullineaux, The rpaC gene product regulates phycobilisome-photosystem II interaction in cyanobacteria, Biochim Biophys Acta, 1709 (2005) 58-68.
[60] C.W. Mullineaux, D. Emlyn-Jones, State transitions: an example of acclimation to low-light stress, J Exp Bot, 56 (2005) 389-393.

[61] S. Joshua, C.W. Mullineaux, The rpaC gene product regulates phycobilisome-photosystem II interaction in cyanobacteria, Biochimica et Biophysica Acta (BBA) - Bioenergetics, 1709 (2005) 58-68.
[62] V. Chukhutsina, L. Bersanini, E.M. Aro, H. van Amerongen, Cyanobacterial Light-Harvesting Phycobilisomes Uncouple From Photosystem I During Dark-To-Light Transitions, Scientific reports, 5 (2015) 14193.

S. elongatus	**Light Intensity**		
	Low	**Intermediate**	**High**
WT	1.46 ± 0.05	2.35 ± 0.17	8.99 ± 0.82
ΔapcD	0.94 ± 0.22*	1.87 ± 0.22*	6.30 ± 0.76*
WT	1.70 ± 0.24	2.79 ± 0.13	7.31 ± 0.41
ΔapcF	1.57 ± 0.28	2.77 ± 0.52	6.93 ± 0.93
Synechocystis	**Light Intensity**		
	Low	**Intermediate**	**High**
WT	0.75 ± 0.12	1.08 ± 0.08	11.43 ± 3.08
ΔapcD	0.73 ± 0.10	0.92 ± 0.08	10.77 ± 1.19
WT	0.87 ± 0.05	2.62 ± 0.10	13.89 ± 0.03
ΔapcF	0.77 ± 0.04*	1.89 ± 0.01*	9.24 ± 0.37*

Table I. Initial rates of P700 oxidation kinetics in *S. elongatus* and *Synechocystis* WT, ΔApcD and ΔApcF strains under orange light illumination. The rates were determined using a linear fit. The mean and the standard deviation of at least three biological independent experiments are shown. The values are expressed in absorbance (rel units).sec^{-1}. * indicates significant differences (Student´s test, $p<0.05$) between WT and mutant strains, for each strain and in each light condition, respectively. Measurements were performed by pairs (each mutant was measured each time with the WT).

	S. elongatus	***Synechocystis***
	$\mathbf{F_{vb}/F_{vd}}$	$\mathbf{F_{vb}/F_{vd}}$
WT	4.72 ± 0.85^{a}	1.24 ± 0.03^{a}
ΔapcD	4.94 ± 0.22^{a}	1.01 ± 0.03^{b}
ΔapcF	5.31 ± 0.45^{a}	1.12 ± 0.03^{c}

Table II. **Fluorescence parameters of *S. elongatus* and *Synechocystis* obtained from a PAM fluorimeter.** The meaning of each parameter is defined in Materials and Methods. All the values (± SD) are the average of at least 4 biological independent experiments. Values without common letters differ significantly within each strain (Tukey test, $p < 0.05$).

Figure 1. The model of *Synechocystis* PCC 6803 (A) and *Synechococcus elongatus* PCC 7942 (B) phycobilisomes. In these strains, the PBSs are constituted by a tricylindric (Synechocystis) or a bicylindric core (*S. elongatus*) surrounded by six rods. Each rod is formed by three hexamers of blue phycocyanin (PC). The rods are stabilized by non-chromophorylated linker proteins (in green). The rod-core linker (LRC) protein (small cylinder in green) stabilizes the binding of the rods to the core. In *Synechocystis* the upper core cylinder is formed by 4 trimers of allophycocyanin (APC), composed by a αAPC–βAPC heterodimer which binds two phycocyanobilins (maximal fluorescence 660 nm). In addition, 2 core linker (Lc) proteins (in red) present in the external trimers stabilize each cylinder. In both strains, in both basal cylinders, in one of the external trimers (in violet in C), one αAPC subunit is replaced by a special αAPC-like subunit called ApcD. In the adjacent trimer (in orange in C), a βAPC-like subunit named ApcF replaces one β-subunit, and another dimer is formed by a β-APC subunit and the bilin-linker domain of an αAPC-like domain (ApcE). The bilins attached to ApcF and ApcE are close (20 Å) and have big influences one on the other. Both ApcD and ApcF/ApcE proteins were described as terminal energy acceptors of the PBS, presenting a maximal fluorescence at 680 nm. In (D) the X-ray tridimensional structure of the APC trimer containing ApcD is shown. The pdb file used in (D) was 4PO5.

Figure 2. Absorbance and room temperature fluorescence emission spectra of *S. elongatus* (A and C, respectively) and *Synechocystis* (B and D, respectively) strains. (A and B) Absorbance spectra measurements were recorded at a Chl concentration of 2.5 µg/mL. (C and D) Room temperature fluorescence spectra of dark-adapted (15 min) cells were recorded at a phycocyanin concentration of 1 µM. Black lines, WT strains; red lines, ΔApcD strains; blue lines, ΔApcF strains. The curves shown are the average of three biological replicates. The excitation wavelength was 590 nm.

Figure 3. Chlorophyll *a* fluorescence induction transients. Measurements were done in *S. elongatus* (A) and *Synechocystis* (B) WT, ΔApcD and ΔApcF strains (black, red and blue lines, respectively). Cells (2.5 µg Chl /mL) were dark-adapted to state II for 15 min before the measurements, and the following inhibitors were added subsequently: 10 µM DCMU and 20 µM DBMIB. Measurements were done with orange actinic light (35 µmol photons m^{-2} s^{-1}) and blue measuring light. The detection wavelength was ≥ 695 nm (far-red). The curves are the average of at least 3 independent biological experiments. The errors bars correspond to the

standard deviation of the data shown. Insets shows the first 0.01 s of each measurement on a linear scale.

Figure 4. P700 oxidation absorption kinetics under orange illumination of *S. elongatus* and *Synechocystis* ΔApcD and ΔApcF mutants. Whole cells (2.5 µg Chl /mL) were dark adapted to state II for 15 min before the measurements. Then the following inhibitors were added subsequently: 15 µM DCMU, 300 µM MV and (after 10 min) 100 µM DBMIB. Orange actinic light, at an intensity of 50 µmol photons m^{-2} s^{-1} (circles), 100 µmol photons m^{-2} s^{-1} (squares) and 200 µmol photons m^{-2} s^{-1} (triangles) were used for *S. elongatus* (A and C). Regarding *Synechocystis* strains, 5 µmol photons m^{-2} s^{-1} (circles), 7 µmol photons m^{-2} s^{-1} (squares) and 50 µmol photons m^{-2} s^{-1} (triangles) were used when the ΔapcD mutant was tested (B), while 6 µmol photons m^{-2} s^{-1} (circles), 8 µmol photons m^{-2} s^{-1} (squares) and 50 µmol photons m^{-2} s^{-1} (triangles) were used in the case of the ΔapcF mutant (D). WT strains are shown in black and the mutant strains in red. At least three biological independent experiments have been measured and the mean trace for each strain is shown.

Figure 5. State transitions in WT and mutants of *S. elongatus* and *Synechocystis*. The fluorescence changes were followed by a PAM fluorimeter. Dark adapted cells (2.5 µg Chl/mL) were successively illuminated with blue (85 µmol photons m^{-2} s^{-1}) and orange (20 µmol photons m^{-2} s^{-1}) light. Saturating pulses (400 ms x 1200 µmol photons m^{-2} s^{-1}) were applied each 90 sec. Typical experiments are shown. (A and B) *S. elongatus* and *Synechocystis* WT, respectively; (C and D) *S. elongatus* and *Synechocystis* ΔapcD, respectively; (E and F) *S. elongatus* and *Synechocystis* ΔapcF, respectively.

Figure 6. State transitions in WT and mutants of *S. elongatus*. 77 K fluorescence emission spectra of dark (black, State II) and blue-light (red, 85 µmol photons m-2 s-1, State I) adapted WT (A and B), ΔapcD (C and D) and ΔapcF (E and F) cells. The excitation was done at 430 nm (A, C and E) or 590 nm (B, D and F). Normalization was done at 800 nm, and the spectra are the average of at least 3 biological independent experiments. The measurements were done at a chlorophyll concentration of 5 µg/mL.

Figure 7. State transitions in WT and mutants of *Synechocystis*. 77 K fluorescence emission spectra of dark (black, State II) and blue-light (red, 85 µmol photons m^{-2} s^{-1}, State I) adapted WT (A and B), ΔapcD (C and D) and ΔapcF (E and F) cells. The excitation was done

at 430 nm (A, C and E) or 590 nm (B, D and F). Normalization was done at 800 nm, and the spectra are the average of at least 3 biological independent experiments. The measurements were done at a chlorophyll concentration of 5 μg/mL.

Highlights:

- **ApcD deletion in *S. elongatus* does not impair state transitions.**
- **Lack of ApcD decreases energy transfer from PBSs to PSI in *S. elongatus.***
- **ApcF deletion decreases energy transfer from PBSs to PSII and PSI in *Synechocystis*.**
- **PBS involvement in state transition might differ in *S.elongatus* and *Synechocystis*.**

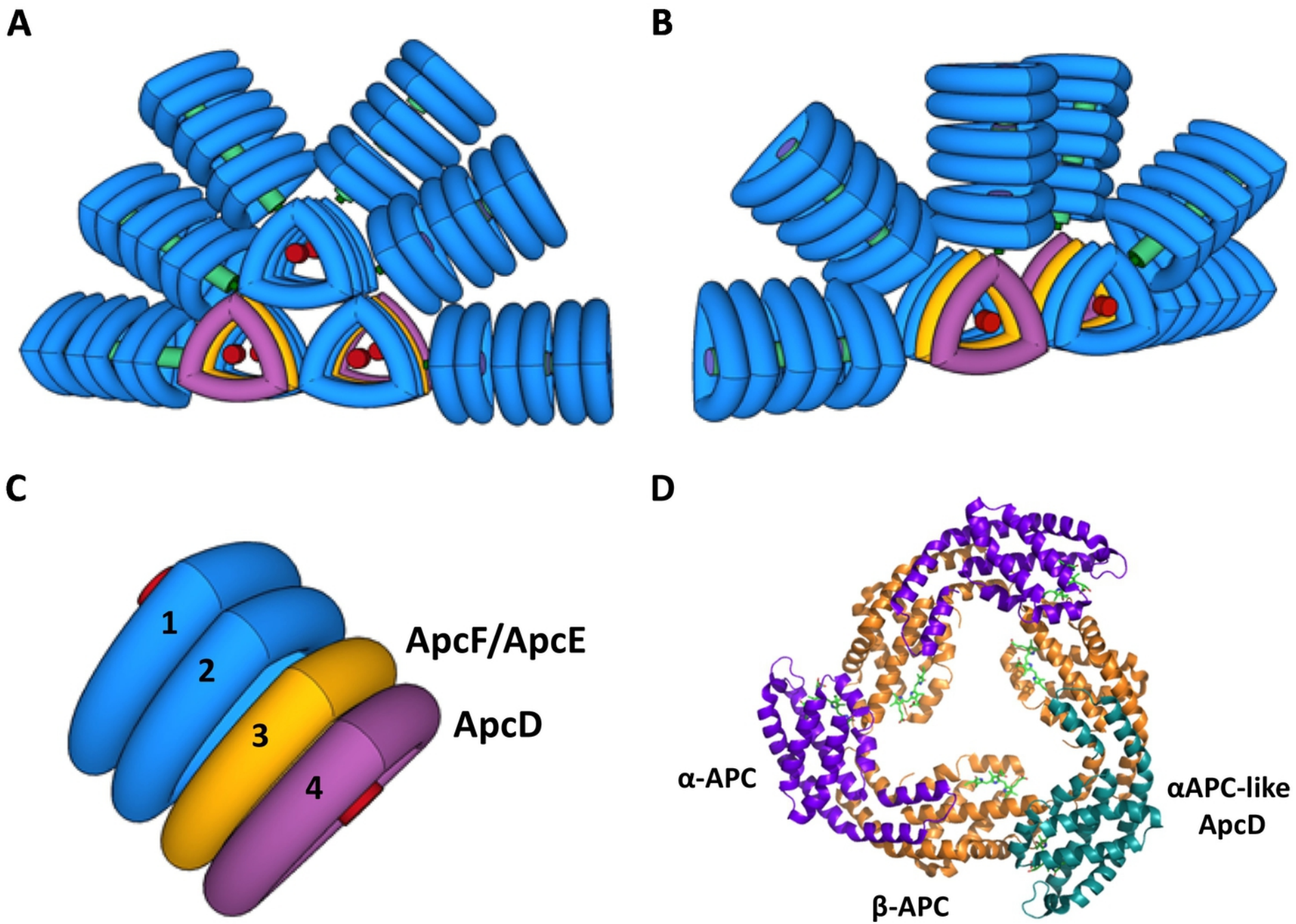

Figure 1

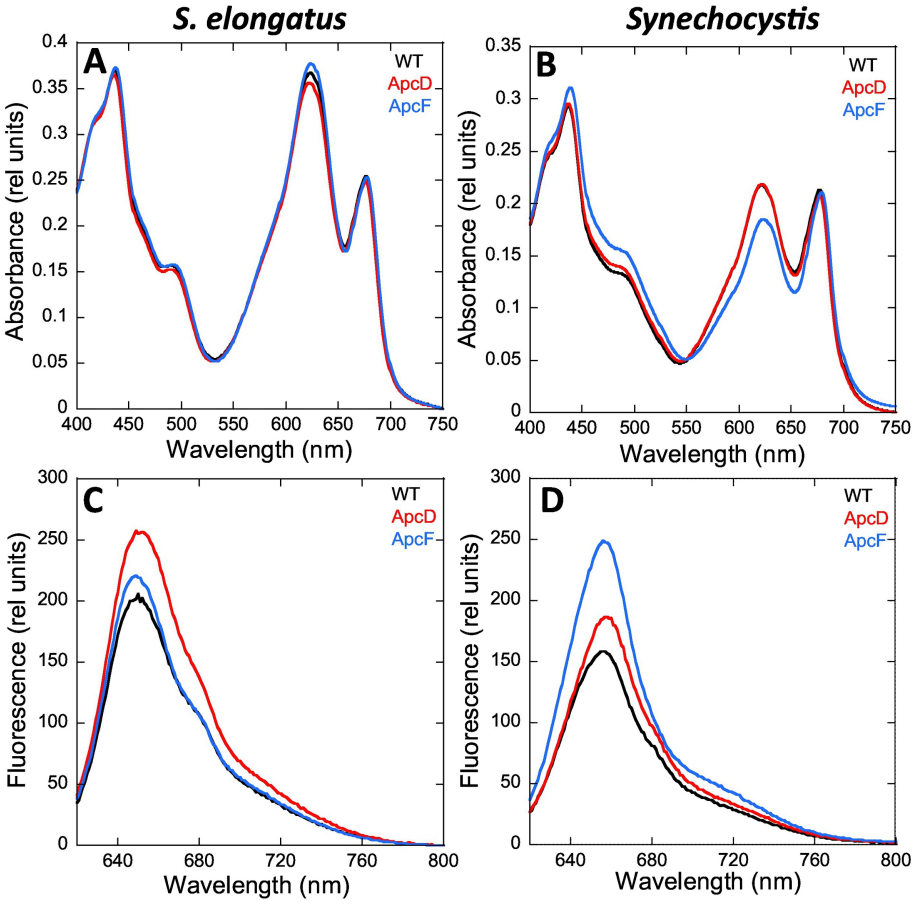
S. elongatus
Synechocystis
A
B
C
D
WT
ApcD
ApcF
Absorbance (rel units)
Fluorescence (rel units)
Wavelength (nm)

Figure 2

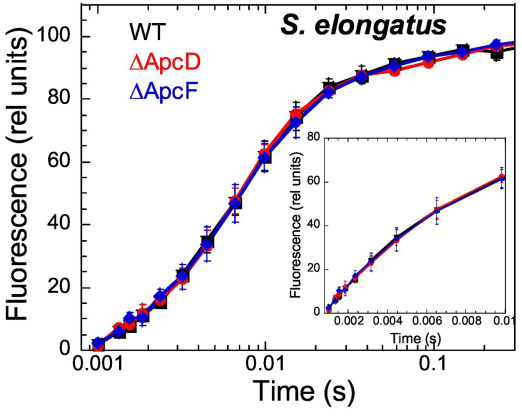
S. elongatus
WT
ΔApcD
ΔApcF
Fluorescence (rel units)
Time (s)
0.001
0.01
0.1
0
20
40
60
80
100
0.002
0.004
0.006
0.008
0.01

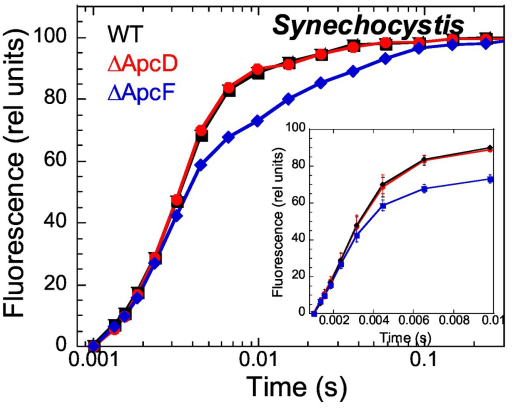
Synechocystis
WT
ΔApcD
ΔApcF
Fluorescence (rel units)
Time (s)
0.001
0.01
0.1
0
20
40
60
80
100
0.002
0.004
0.006
0.008
0.01

Figure 3

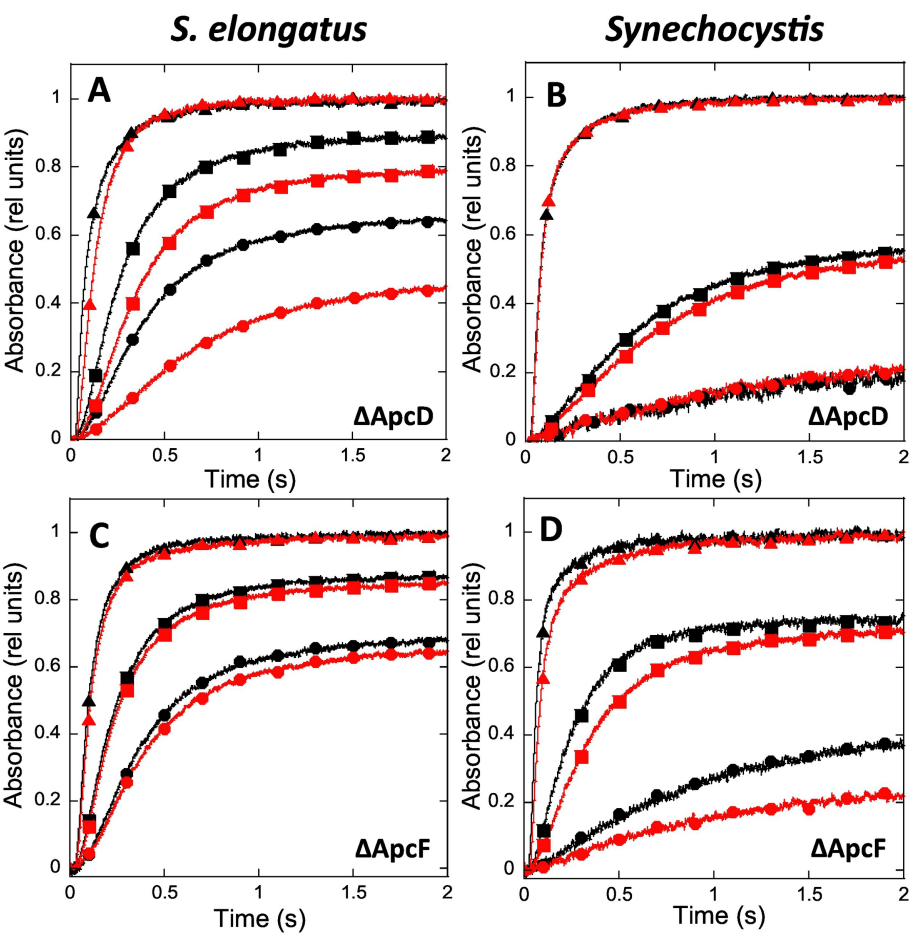
S. elongatus
Synechocystis
A
B
C
D
ΔApcD
ΔApcD
ΔApcF
ΔApcF
Absorbance (rel units)
Time (s)
0
0.2
0.4
0.6
0.8
1
0.5
1.5
2

Figure 4

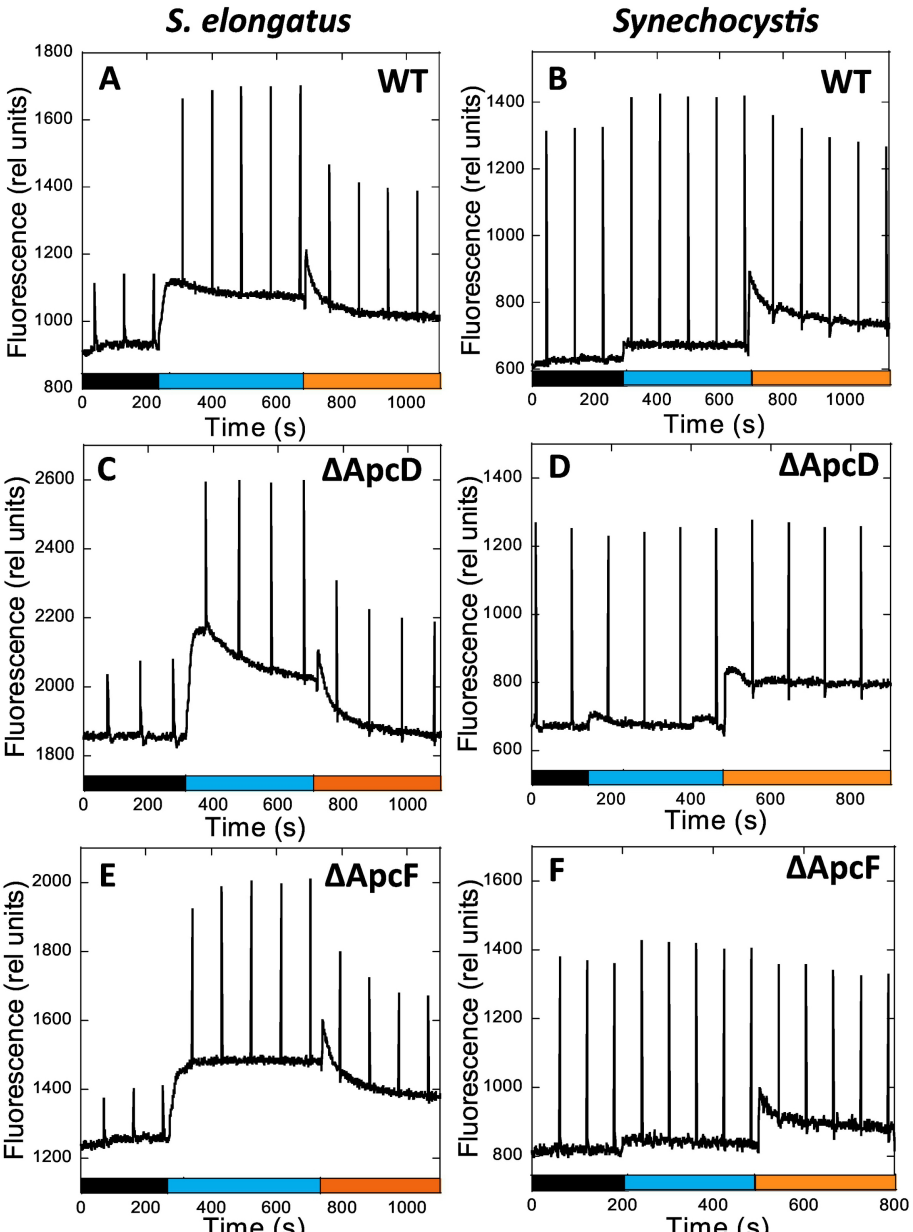
S. elongatus
Synechocystis
A
WT
B
WT
C
ΔApcD
D
ΔApcD
E
ΔApcF
F
ΔApcF
Fluorescence (rel units)
Time (s)

Figure 5

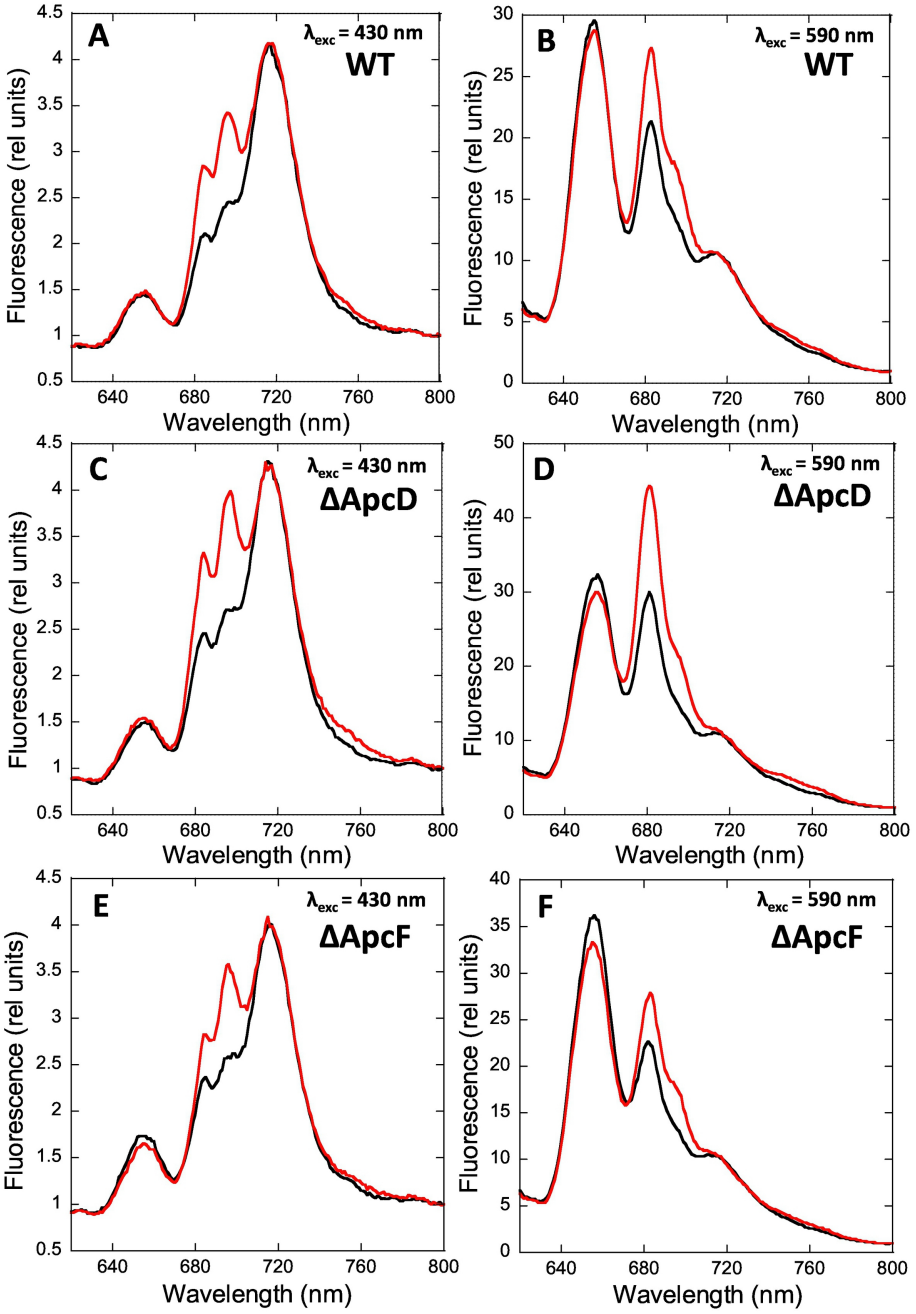
A
λexc = 430 nm
WT
B
λexc = 590 nm
WT
C
λexc = 430 nm
ΔApcD
D
λexc = 590 nm
ΔApcD
E
λexc = 430 nm
ΔApcF
F
λexc = 590 nm
ΔApcF
Fluorescence (rel units)
Wavelength (nm)

Figure 6

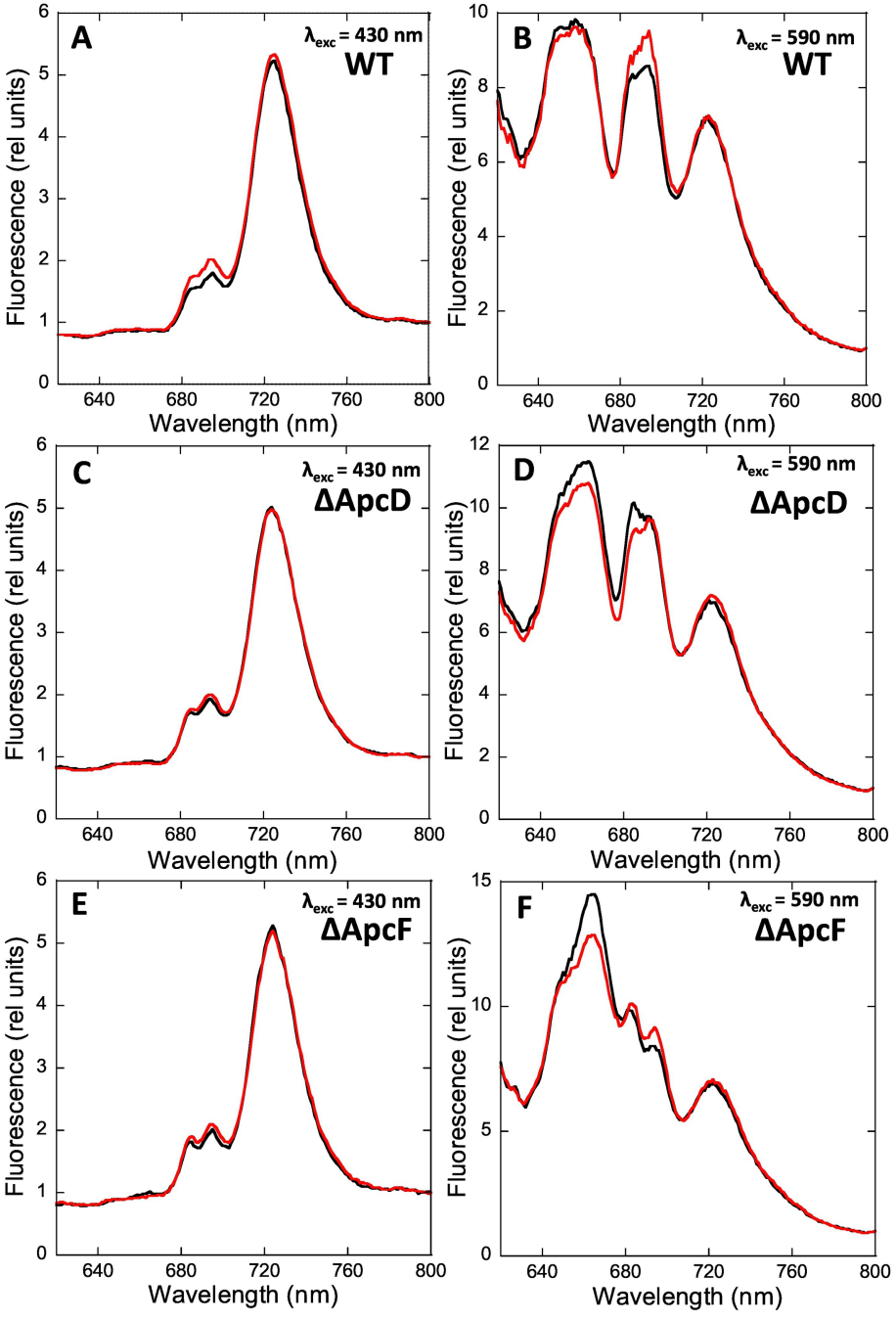
A
λexc = 430 nm
WT
B
λexc = 590 nm
WT
C
λexc = 430 nm
ΔApcD
D
λexc = 590 nm
ΔApcD
E
λexc = 430 nm
ΔApcF
F
λexc = 590 nm
ΔApcF
Fluorescence (rel units)
Wavelength (nm)

Figure 7